Graphene oxide cross-linked chitosan-based hydrogel:- Synthesis, Characterization and Rheological behavior

Mehnaz Ayoub[1*], Shakeel Ahmad Rather[2], Erma Aijaz, Hina Sajad

1. Department of Chemistry, School of Chemical Engineering and Physical Science, Lovely Professional University, Phagwara Punjab, India (144411)

2. Department of Civil Engineering, Dr B R Ambedkar National Institute of Technology Jalandhar

* Email:- mwani9625@gmail.com

Abstract

The abstract highlights the synthesis and characterization of a dual cross-linked and highly stretchable hydrogel derived from graphene oxide-modified chitosan (CS). Various hydrogel samples were created, each featuring different concentrations of graphene oxide (GO) and utilizing glutaraldehyde (GD) as a covalent cross-linker. To characterize these hydrogels, several experimental techniques were employed, including Fourier transform infrared (FTIR), Thermo gravimetric analysis (TGA), and Scanning electron microscopy (SEM). The TGA analysis exhibited the enhanced stability of CS-GD-GO in comparison to CS-GD hydrogel, indicating superior thermal properties conferred by the incorporation of graphene oxide. The structural behavior was investigated using rheological measurements, where hydrogels with varying graphene oxide concentrations underwent analysis through vibrational frequency sweep and strain sweep conditions. The rheological studies unveiled an increase in elastic parameters, such as storage modulus and viscosity, correlating with heightened graphene oxide concentrations. Additionally, the hydrogels demonstrated shear thinning and shearing thickening behaviors, showcasing an augmentation with escalating shear rates. Moreover, the hydrogels' self-healing capability was confirmed through stepwise dynamic strain measurements, indicating their potential for restoration and resilience under mechanical stress. The abstract further emphasizes the potential applications of these hydrogels due to their porous structure, ideal for tasks like the separation and adsorption of metal ions and organic dyes. Overall, the synthesized hydrogels exhibit promising properties, including enhanced stability, tunable viscoelastic behavior, and self-healing characteristics, rendering them suitable for various practical applications in fields such as environmental remediation and separation technologies.

Keywords

Hydrogel, graphene oxide, chitosan, cross-linker

Introduction

Hydrogels constitute a category of polymeric materials renowned for their remarkable ability to retain substantial amounts of water within a three-dimensional network [1]. These versatile materials find extensive applications across diverse industries and in various medical products. The existence of hydrogels in nature dates back to the origins of life on Earth, exemplified by bacterial biofilms and plant structures that exhibit water-induced swellings [2]. Throughout human history, the early utilization of substances like gelatin and agar underscored the foundational understanding of hydrogels [3]. However, the precise classification and development of hydrogels as a distinct class of polymers primarily emerged in contemporary times, specifically tailored for biomedical applications [4]. Notably, the pivotal discovery in 1936 by scientist Dupont, regarding the synthesis of methacrylic polymers and the mention of poly (2-hydroxyethyl methacrylate) {poly HEMA}, marks a significant milestone in the evolution of hydrogel science. While chemically stable, hydrogels possess the inherent property of eventual degradation, dissolution, and disintegration [5]. This characteristic, coupled with their well-documented low toxicity, biocompatibility, and susceptibility to degradation by human enzymes, propelled significant interest in hydrogels crafted from natural polymers like chitosan [6-7]. Chitosan, renowned for its bioadhesive, bacteriostatic, hemostatic, and antioxidant properties, has garnered considerable attention as a versatile biomaterial [9-12]. Its structural adaptability offers a diverse array of functional possibilities, making it an attractive candidate for applications in drug delivery, tissue engineering, wound dressing, and various biomedical fields [13-15]. The intermolecular forces governing chitosan, including hydrogen, hydrophobic, and ionic interactions, significantly contribute to the stability and integrity of the cross-linked hydrogel structure, preventing the breakdown of cross-links during swelling [16-19]. Moreover, chitosan hydrogels exhibit suitability in constructing bone and cartilage, showcasing their versatility and adaptability for regenerative medicine purposes. Their responsiveness to environmental stimuli positions them as intelligent materials applicable in both in vivo and in vitro scenarios [20–22]. The promising characteristics of chitosan-based systems open up a broad spectrum of potential applications across diverse disciplines such as molecular biology, nanomedicine, and medical technology, offering immense promise for future advancements and innovations.

In our research, we placed a strong emphasis on developing a wide array of chitosan-based hydrogel samples. Our main objective was to deliberately manipulate the viscoelastic traits of chitosan (CS) by introducing dual crosslinkers, namely GD and GO. Our comprehensive

investigation centered on unraveling the intricate rheological qualities inherent in these hydrogels, unveiling their exceptional attributes concerning viscosity and elastic modulus. This thorough understanding empowered us with precise tools to fine-tune and govern the mechanical behavior of chitosan-based hydrogels, a pivotal aspect for their adaptable usage across various applications. Furthermore, employing scanning electron microscopy (SEM) allowed us to delve deeper into the structural aspects. We discovered a markedly porous surface upon the incorporation of GO, a characteristic that holds immense significance for numerous practical applications. This particular surface property proves instrumental in diverse fields such as the absorption of dyes, capture of polyaromatic hydrocarbons, and sequestration of heavy metals. An outstanding result of our approach was the creation of a highly stretchable system, a consequence of achieving reversible interactions within the hydrogel structure. This unique feature significantly enhances the material's flexibility and adaptability to varying conditions. In summary, our research findings present these chitosan-based hydrogels as promising candidates for multifaceted applications owing to their tailor-made mechanical properties and distinct surface characteristics. This highlights their potential for addressing challenges across a wide spectrum of fields and industries details

Experimental Details

Material

In the research methodology, Chitosan with an average molecular weight of 100,000 and a degree of deacetylation of 79.1% was employed. The Glutaraldehyde solution utilized (25% concentration) was procured from Sigma Aldrich and utilized as provided. Additionally, the chemicals used in the study included Graphite powder, Sulphuric Acid, Phosphoric Acid, Potassium Permanganate, Hydrogen Peroxide, Hydrochloric Acid, Deionised Water, and Glacial Acetic Acid (99.95% purity), all supplied by Merck. Notably, all these chemicals were of analytical reagent grade, ensuring a high standard of purity and quality required for the precise execution of the experimental procedures. The use of specific materials and chemicals from reputable suppliers ensures the reliability and reproducibility of the experimental outcomes, establishing a robust foundation for the scientific investigations conducted in the study.

Synthesis of Graphene oxide

Graphene Oxide (GO) was synthesized through a modified Hummers method starting from pure graphite powder. The process commenced by mixing 27 ml of sulfuric acid (H_2SO_4) and

3.0 ml of phosphoric acid (H_3PO_4) in a volume ratio 9:1, followed by stirring the solution for several minutes. Subsequently, a slow addition of 1.32 g of potassium permanganate ($KMnO_4$) ensued. This mixture was continuously stirred for 6 hours until the solution exhibited a dark green, indicating the reaction progress. To neutralize excess $KMnO_4$, 0.67 ml of hydrogen peroxide (H_2O_2) was cautiously added, prompting an exothermic reaction, which was allowed to cool down. Upon cooling, a solution containing 10 ml of hydrochloric acid (HCl) and 30 ml of deionized water (DIW) was introduced, and the resultant solution was centrifuged using an Eppendorf Centrifuge 5430 R at 5000 rpm for 7 minutes. Following centrifugation, the supernatant was carefully decanted, leaving behind residual materials that underwent three subsequent washes with HCl and DIW to ensure thorough purification. The resulting washed GO solution was then subjected to drying using an oven set at 90°C for 24 hours, thereby yielding the powdered form of Graphene Oxide. This meticulous process of synthesis and purification ensures the production of high-quality GO powder, essential for various applications and research endeavors involving graphene-based materials.

Synthesis of Chitosan Glutaraldehyde Graphene Oxide Hydrogel (CS-GD-GO)

The creation of CS-GD-GO gel involved a methodical procedure. It commenced by dissolving 0.10 grams of chitosan in a 6ml solution of 2% acetic acid. This chitosan solution was allowed to stand overnight to ensure the proper formation and dissolution of chitosan within the solution. Following an 18-hour duration, 2.0 ml of an 8% glutaraldehyde solution, functioning as the cross-linking agent, was introduced to each sample. Concurrently, varying amounts of graphene oxide were added to the solution to achieve a total volume of 11.0 ml per sample. The specific quantities of glutaraldehyde solution employed in each sample are detailed in Table 1, delineating the variations among the samples. Subsequently, the CS-GD-GO gels, once prepared, underwent a drying process through freeze-drying to preserve their structural integrity and composition. Once the gels were adequately dried, the samples were forwarded for comprehensive characterization, wherein their physical, chemical, and structural attributes were meticulously examined and analyzed**.** This systematic approach ensured the creation of CS-GD-GO gels with controlled variations in their composition, particularly concerning the levels of glutaraldehyde and graphene oxide. The subsequent characterization process aimed to discern and understand the resulting properties and behaviors of these gels, critical for determining their potential applications in diverse scientific and industrial fields.

Table 1:- Synthesis of Chitosan Gluteraldehyde Graphene oxide Hydrogel

S.No.	Chitosan	Acetic Acid	Gluteraldehyde	Graphene oxide	Water
1.	0.1g	6.0ml	0.0ml	0.0ml	5.0ml
2.	0.1g	6.0ml	2.0ml	0.0ml	3.0ml
3.	0.1g	6.0ml	2.0ml	0.5ml	2.5ml
4.	0.1g	6.0ml	2.0ml	2.5ml	0.5ml
5.	0.1g	6.0ml	0.0ml	3.0ml	2.0ml

Result and Discussion

Hydrogels,formed from smart materials, exhibit a diverse spectrum of advantageous properties, including self-healing capabilities, robust mechanical strength, and responsiveness to external stimuli. These characteristics render them highly promising for a myriad of applications within biomedical science and materials science. This specific study aimed to synthesize and characterize a GO based hydrogel by utilizing CS as the primary polymer backbone and GD as the cross-linker. Distinct samples (S1-S5) were meticulously crafted with the intent to augment the viscoelastic behavior of the hydrogel. In the initial sample (Sample 1), 10.01 grams of chitosan were dissolved in a 6ml solution of 2% acetic acid and left overnight to facilitate the formation of a chitosan hydrogel characterized by a comparatively lower storage modulus (G'). Subsequently, in Sample 2, the addition of an 8% GD solution, serving as a cross-linking agent, led to a remarkable enhancement in the G' value and overall mechanical and viscoelastic properties compared to the chitosan hydrogel formed solely with CS. The subsequent creation of Samples 3 and 4 involved an escalation in the graphene oxide concentration. This deliberate increase aimed to bolster the hydrogel's thermal stability, storage modulus, and sorption capacity by leveraging the augmented surface area arising from heightened porosity, as visually depicted in Figure 3.4. Correspondingly, an increase in viscoelastic properties was observed, as illustrated in Figure 3.6, corroborating the hydrogel's self-healing attributes through stepwise dynamic strain measurements. Sample 5's distinctive feature lay in the augmentation of G' values via ionic cross-linking between chitosan and graphene oxide. This innovation resulted in a highly modified system, manifesting augmented property dispositions within GO-based hydrogels. These advanced hydrogels demonstrate significant potential across diverse applications, including the efficient adsorption of metal ions, and polyaromatic hydrocarbons, and the effective removal of dyes from various environments. The successful development and

characterization of these highly tailored hydrogels underscore their promising role in addressing multifaceted challenges, offering versatile solutions across a wide array of scientific, industrial, and environmental applications.

Table 2:- Modulation of storage modulus in CS-GD-GO Hydrogel

Sample No.	Chitosan	Acetic Acid	Glutaraldehyde	Graphene oxide	Water	Remarks (G' value)
Sample 1.	0.1g	6.0ml	0.0ml	0.0ml	5.0ml	Very Low
Sample 2.	0.1g	6.0ml	2.0ml	0.0ml	3.0ml	Low
Sample 3.	0.1g	6.0ml	2.0ml	0.5ml	2.5ml	Moderate
Sample 4.	0.1g	6.0ml	2.0ml	2.5ml	0.5ml	High
Sample 5.	0.1g	6.0ml	0.0ml	3.0ml	2.0ml	Very High

Fourier-transform infrared spectroscopy (FTIR) Analysis

FTIR analysis depicted in Figure 1 presents significant insights into the structural alterations occurring within the materials under examination. The spectrum (Figure 1(a)) representing pure chitosan showcases characteristic peaks at specific wavenumbers: 1592 cm^{-1} denotes the amino group, while 3429 cm^{-1} signifies the hydroxyl group. Additionally, a discernible peak at 1656 cm^{-1} corresponds to the carbonyl stretching vibration of the residual acetamide group within the chitosan structure. In contrast, Figure 1(b) demonstrates a substantial alteration in the spectrum after the cross-linking reaction. A prominent and robust peak at 1558.48 cm^{-1} becomes apparent, indicative of the imine bond (C=N) formation resulting from the interaction between the aldehyde group present in GD and the amino groups inherent in CS. This distinctive peak serves as compelling evidence supporting the creation of a Schiff base, thereby confirming the successful cross-linking between GD and CS. After the cross-linking process, Figure 1(c) showcases alterations in the spectral features, notably emphasizing the strengthened and slightly shifted peak corresponding to the ether group. The transition from 1027 cm^{-1} to 1068.57 cm^{-1} indicates the presence and formation of newly created open-chain ether bonds within the hydrogel structure. This shift and reinforcement of the ether group peak signify the

establishment of these specific chemical bonds post-cross-linking, further corroborating the structural modifications occurring within the hydrogel matrix. Moreover, the confirmation of the presence of GO in the composite material is deduced through the examination of its surface morphology, elucidating the characteristic features associated with GO within the synthesized material. This complementary analysis augments the FTIR findings, providing comprehensive evidence of the incorporation of GO into the hydrogel matrix. In essence, the FTIR spectral analysis offers a detailed understanding of the molecular transformations and intermolecular interactions taking place within the synthesized materials, providing crucial evidence supporting the successful formation of specific chemical bonds, cross-linking reactions, and the integration of graphene oxide within the hydrogel structure.

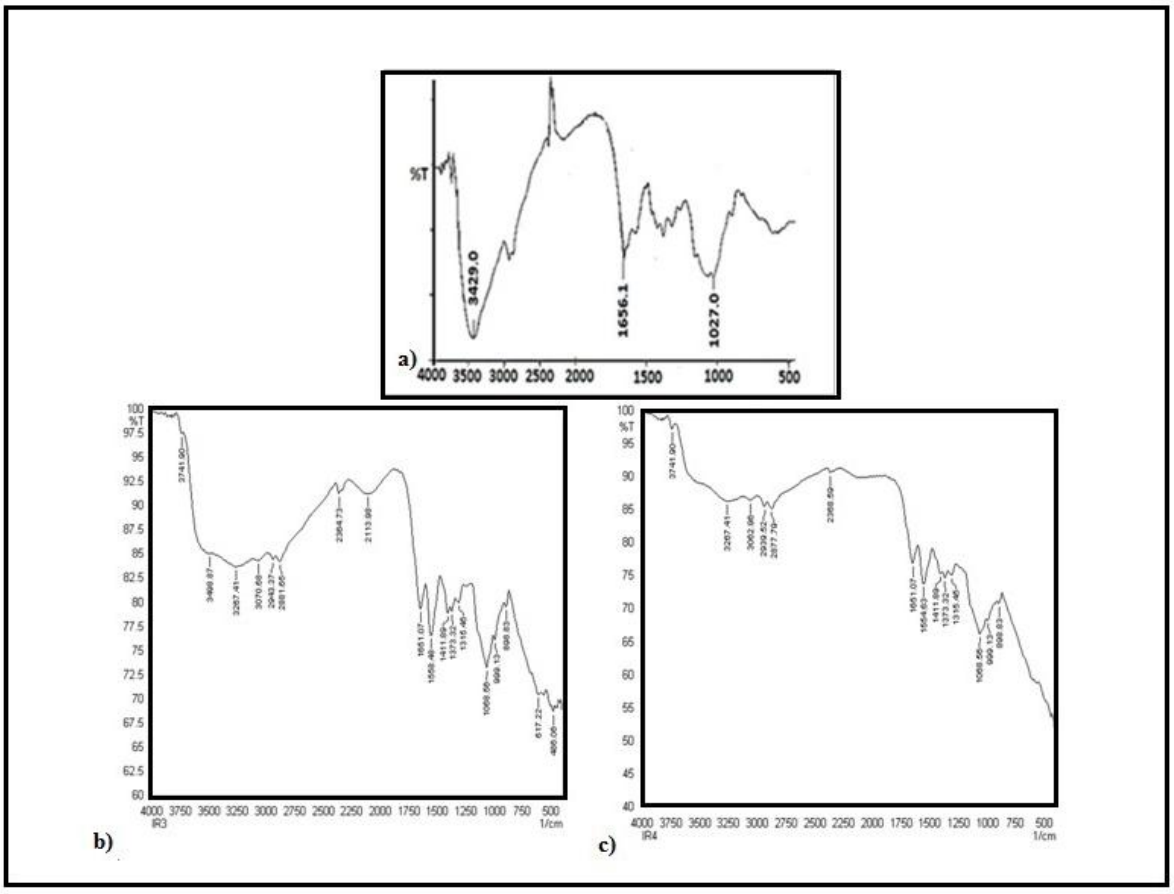

Figure 1:- Absorption spectrum of (a) CS only (b) CS-GD (c) CS-GD-GO

Thermogravimetric Analysis (TGA)

TGA conducted on the CS-GD material, as depicted in Figure 2 (b), showcases a thermogram exhibiting a typical sigmoidal shape, providing valuable insights into the material's thermal behavior. The plot unveils a sequence of five distinctive peaks, each signifying specific weight loss events during thermal degradation. The initial degradation initiates at 26.53°C and

concludes at 120.0°C, accounting for a weight loss of 16.24%, primarily attributed to dehydration processes. Subsequently, the second degradation phase spans from 120.0°C to 200.0°C, resulting in an 8.36% weight reduction. The third degradation stage occurs between 200°C and 400°C, leading to a substantial weight loss of 44.9%. Following this, the fourth weight loss event transpires from 400°C to 645°C, amounting to approximately 29.85%. Cumulatively, the total weight loss experienced by CS-GD from 26.53°C to 645°C amounts to approximately 99.36%. Figure 2 (d) displays the TGA curves for CS-GD-GO, revealing a similar sigmoidal pattern. Four discernible weight loss peaks are evident in this thermogram. The initial peak commences at 26.11°C and terminates at 120.00°C, causing a weight loss of 17.105% attributed to dehydration processes. The subsequent peak, occurring between 120°C and 195°C, contributes to a 5.545% weight reduction due to hydrogen bonding between CS and GD. The third weight loss event spans from 195°C to 629°C, accounting for a substantial 98.02% weight reduction primarily linked to the decomposition of CS chains. The cumulative weight loss experienced by CS and GD from 26.11°C to 629.39°C totals approximately 98.026%. Comparatively, the observed decrease in weight loss for CS-GD-GO in contrast to CS-GD signifies the higher thermal stability of the former. This distinct disparity in weight loss events indicates the improved resistance to thermal degradation exhibited by the CS-GD-GO composite material. These findings underscore the enhanced thermal stability conferred upon the material by incorporating GO within the CS-GD matrix, offering valuable insights into its potential applications requiring elevated thermal performance.

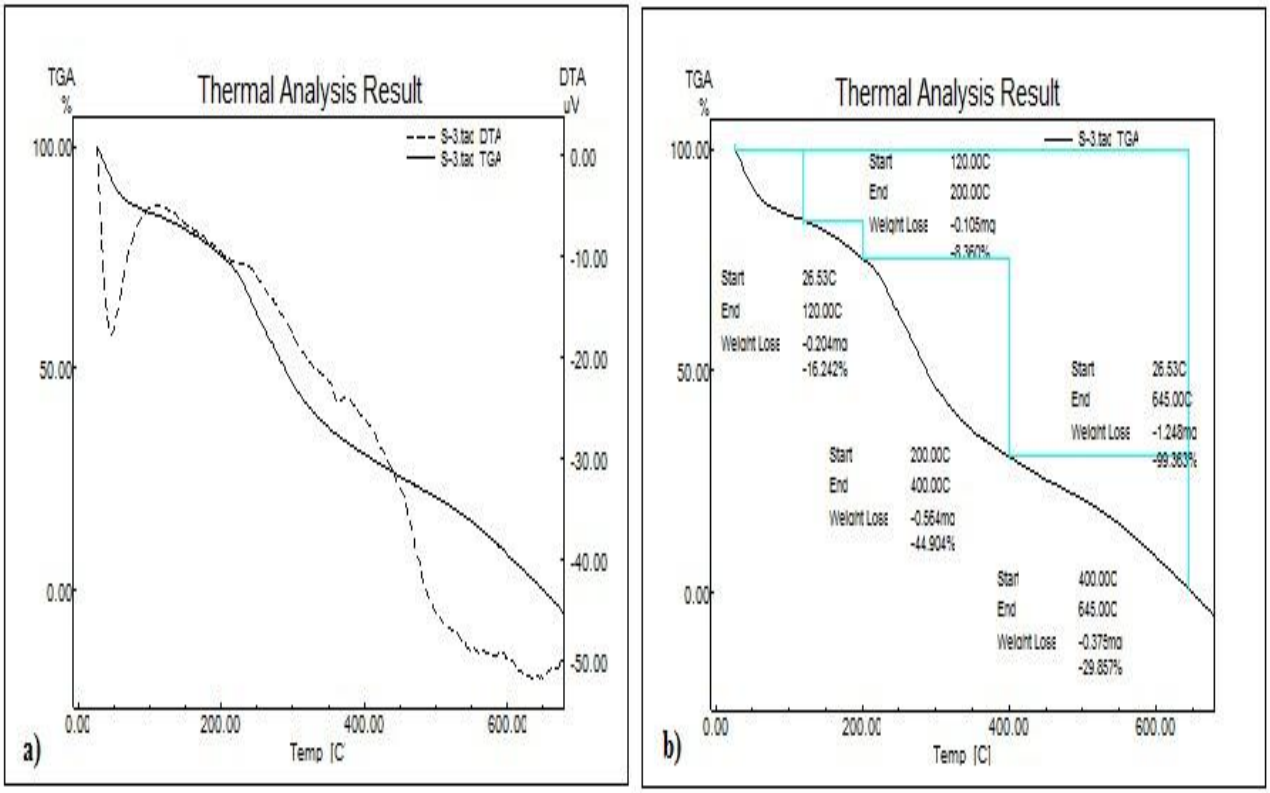

Figure 2:- Thermogram of CS-GD (a and b)

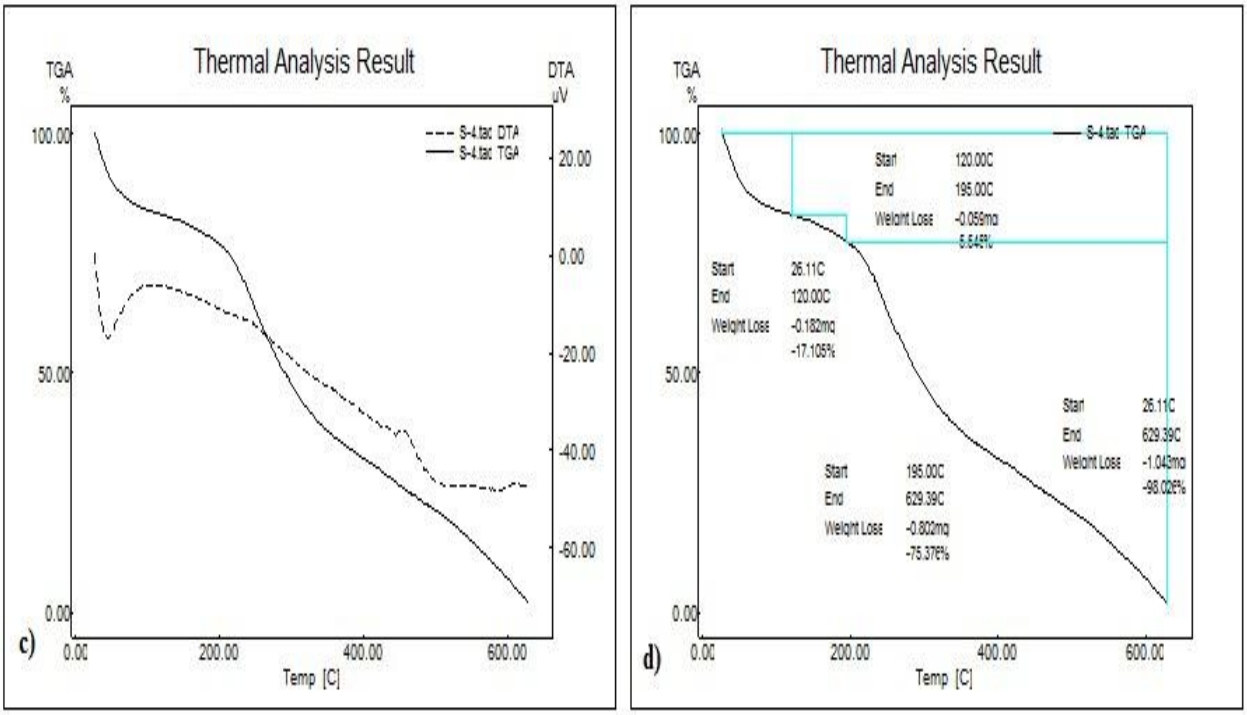

Figure 2:- Thermogram of CS-GD-GO (c and d)

Scanning Electron Microscopy (SEM) Analysis

The SEM images presented in Figure 3 visually depict lyophilized chitosan samples under various conditions, illustrating their morphological characteristics in the presence and absence of GO and the cross-linking agent GD. Figure 3 (a) exhibits the SEM image of CS in its singular form without the presence of a cross-linker. The image portrays a structure that appears less compact and fragmented, indicating a lack of structural integrity attributed to the absence of a cross-linking agent. This visual observation aligns with the expectation that without cross-linking, the chitosan structure would exhibit a less cohesive and organized appearance. Conversely, Figure 3 (b) displays the surface of the chitosan sample when treated with the GD cross-linker. The SEM image depicts a surface exhibiting higher compactness and coherence, clearly indicating the effectiveness of GD as a cross-linking agent. The increased compactness validates the role of GD in facilitating the formation of cross-links within the chitosan matrix, enhancing its structural integrity. Moving to Figure 3 (c), the SEM image showcases a lyophilized CS sample without the presence of GD as a cross-linker. The structure appears as a loose 3D network, revealing interconnected pores within the material. These interconnected pores signify an efficient system for solute diffusion, which is vital for applications involving adsorption processes. Lastly, Figure 3.4(d) presents the network structure in the presence of both GD and GO, constituting a dual cross-linked system. This composite material displays a surface that is less porous compared to the CS sample without GD, indicating a reduction in pore size due to the dual cross-linking effect. However, the incorporation of GO enhances the surface properties, imparting roughness and increasing the surface area of the hydrogel. This augmentation in surface area and roughness attributed to GO addition contributes to reinforcing the strength of the hydrogel, thus indicating its potential for enhanced performance in various applications requiring increased surface characteristics and structural integrity.

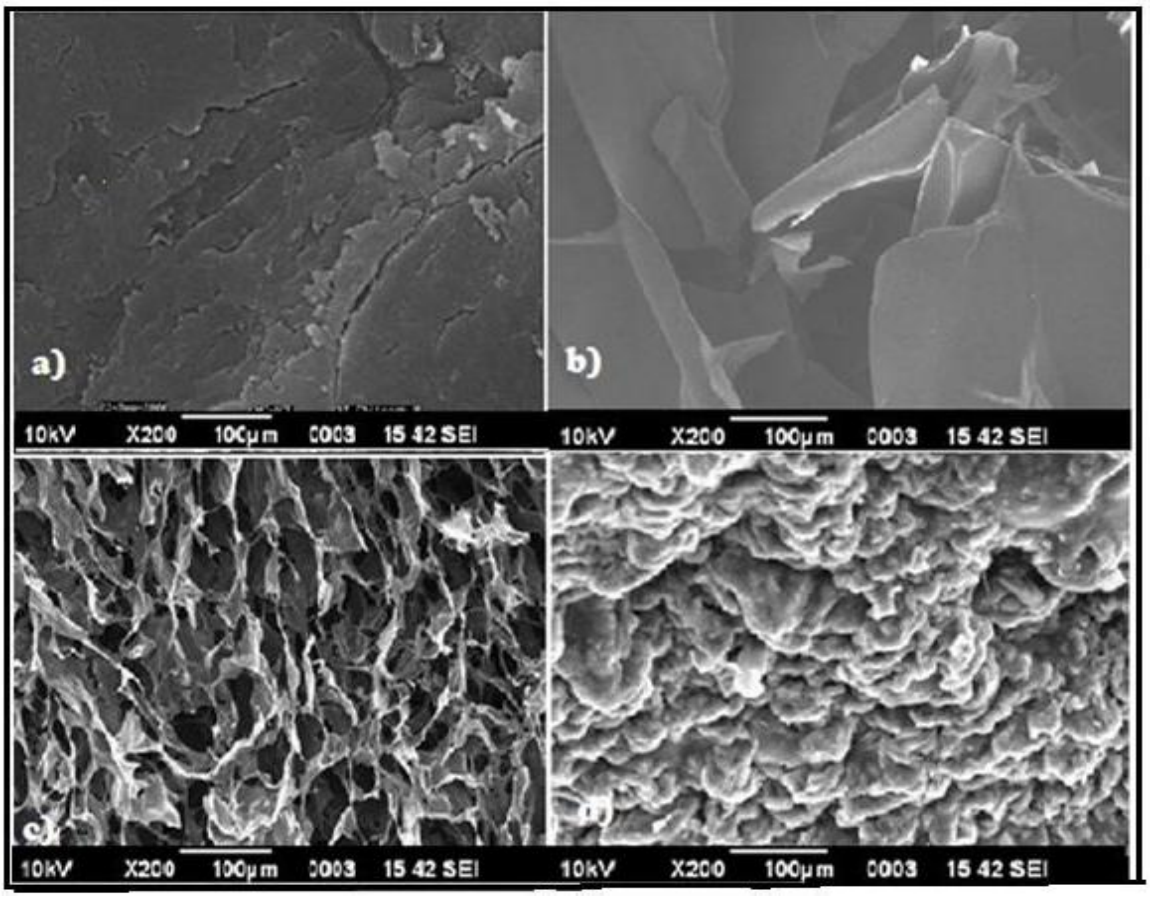

Figure 3:- SEM images of lyophilized hydrogels of (a) CS only (b) CS+GD (2%) (c) CS+GO only (d) CS+GD (2%)+GO

Rheological analysis

The rheological analysis is performed to study the flow behavior of hydrogels and assess the impact of cross-linkers on various parameters. Our research was focused on four key observations. Firstly, we examined the viscosity changes resulting from the addition of GO to CS hydrogels. Secondly, we analyzed the variations in G' and G" values of CS hydrogels after the addition of the GO cross-linker. Additionally, we explored the fluctuations in G' and G" values under different frequency and strain sweep conditions.

Flow Curve

Two types of plots have been observed as shown in Figure 4 (a, b) variation of viscous properties of CS in the presence of only GO. For CS only, it is observed that the hydrogel behaves as Newtonian under low shear rates and does not show any dependence on shear rates. However, at high shear rates, there is shear thinning behavior due to the disruption of a weak polymeric network. The viscosity profile displays a visible increase in the viscosity of CS by

the insertion of GO. It can also be concluded that the amount of crosslinking has increased to a very high extent. The viscosity profile in the presence of GO shows strong network build-up by ionic as well as strong hydrogen bonding interactions between GO and CS. As CS hydrogels are positively charged the –COO- groups of GO do strong crosslinking and as such the GO itself acts as a cross-linker and enhances the stretching behavior of hydrogels as well due to the reversible nature of these interactions. Figure 4 (b) shows characteristic behavioral changes on the addition of GO at the same GD concentrations these systems show Newtonian and Non-Newtonian trends at different shear rates. The Viscosity of CS-GD hydrogel shows increased G' than CS only due to increased cross-linking points due to the formation of imine linkages by the addition of GD. However, CS hydrogels show an unusual response of GO only. The graphs show initially a rise in viscosity after it remains constant and then shear thinning occurs at high shear rates. An increase in viscosity can be attributed to an increase in linkages. However, the constant viscosity region at lower shear rates suggests Newtonian behavior can be attributed to cross-links formed at a rate at which they are broken due to ionic and hydrogen bonding by GO. Further, shear thinning occurs at high shear rates due to disruption of crosslinked networks.

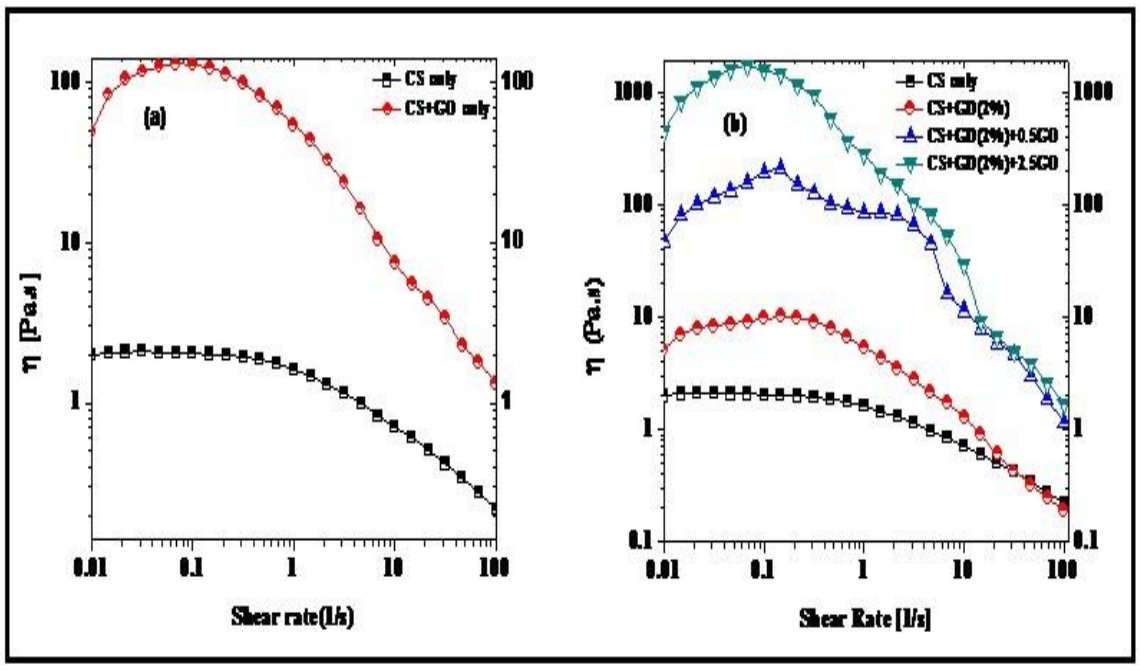

Figure 4 :- (a) Viscosity plots of CS and CS+GO (b) Viscosity plots of CS+GD (2%) and GO

Dynamical mechanical analysis

To determine the self-healing properties of the hydrogel, dynamic mechanical analysis was performed by observing the behavior of the sample when subjected to periodic stress or

deformation fluctuations. Figure 5 confirms that the GO double cross-linked hydrogel exhibits self-healing ability. Dynamic strain scanning measurements of the CS hydrogel system were performed under small (10%) and large (1000%) strains. When subjected to low stress, the G' value is higher, indicating the presence of gel. However, under 1000% strain, the G' value was reversed, indicating that the hydrogel transitioned to a sol state due to a bond fracture between the polymer framework and GO. These findings are consistent with the oscillatory strain sweep measurements. When they are again subjected to 10% pressure, the G' value of the hybrid hydrogel will return to its original state. The CS-GO hydrogel system undergoes a force-induced sol-gel transition by a small deformation that synergizes the polymers to reconstruct the bond between the polymer and the surfactant. Our observations indicate that CS hydrogel systems behave as thixotropic elastic solids that regain their elasticity after the strain is removed. This makes the system a self-healing system over time.

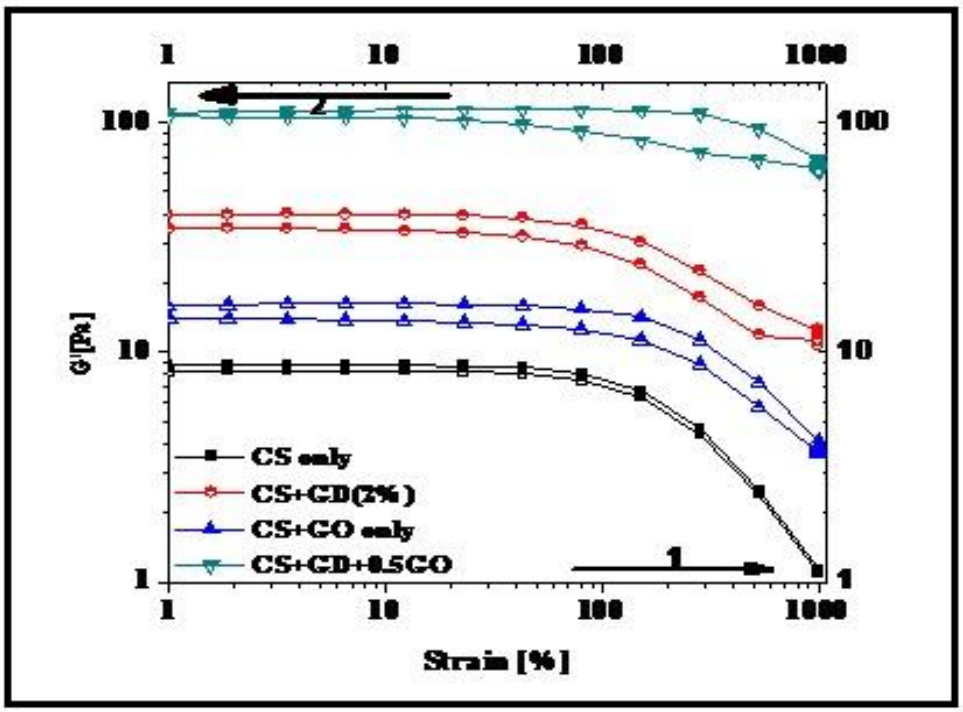

Figure 5:- Dynamic self-healing of CS hydrogel at various GO concentrations

Strain Sweep

The synthesized hydrogel system was analyzed using strain amplitude sweep measurements to determine the storage modulus (G′) and loss modulus (G″). Figure 6 (a-d) shows the crossover between G′ and G″ at 255% strain (critical strain) for the CS hydrogel with and without GD. However, in the presence of GO (2.5), G′ and G″ do not cross over even at 500% (critical strain). With an increase in GO concentration, G′ starts to increase due to a strongly crosslinked

network, which remains unaffected at increasing strain. The cohesion energy, which is involved in the formation of cross-linking between polymer chains, is calculated from the critical strain (above which the behavior becomes non-linear) as

$$EC = 1/2\gamma 2G'C \qquad (1)$$

where c, G′c, and Ec represent the critical strain, storage modulus at critical strain, and cohesion energy, respectively. The cohesive energy values for CS only, CS+GD (2%), CS-GD (2%), +2.5ml, and GO could be calculated at critical strains. The calculated cohesive energy values are approximately 1.02 x 105, 5.96 x 103, 1.88 x 104, and 2.05 x 103 kJ/cm3. At higher GO concentrations, the cohesive energy increases, which can be attributed to the more stabilizing interactions like hydrogen bonding and electrostatic interactions dominating due to the presence of GO. However, at no GO concentration, the breakdown of linkage between polymer chains occurs due to lower cross-linking, which is due to the absence of GO.

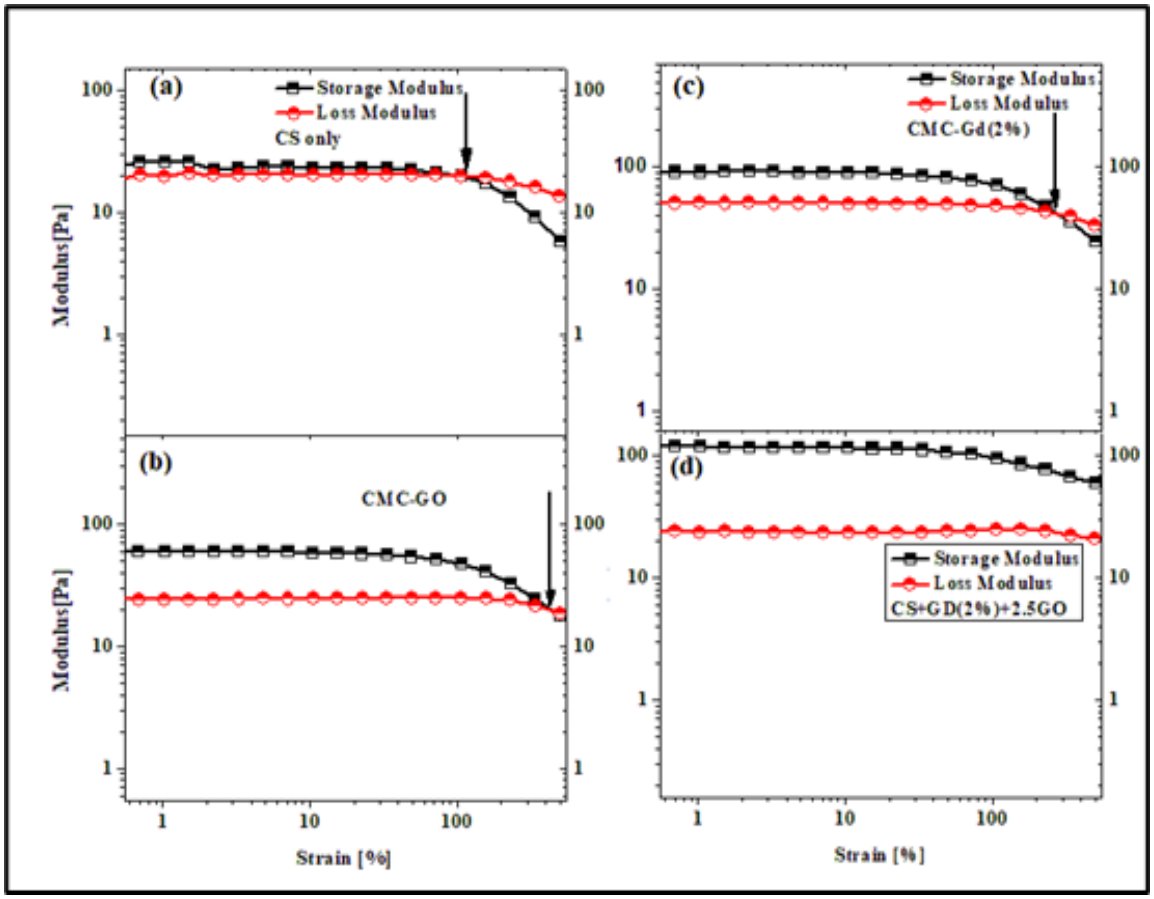

Figure 6:- (a-d) represents the behavior of hydrogel under varying strain conditions (0-500%)

Oscillatory frequency sweep

In Figure 7, we see the frequency sweep plots of CS hydrogels. These plots illustrate how the storage modulus (G') and loss modulus (G'') values change as the frequency varies in the presence of different concentrations of GO at a constant GD concentration. The plots indicate that the G' values are altered as the concentration of GO changes. The storage modulus (G') of different hydrogels at varying GO concentrations is greater than the loss modulus (G") throughout the tested range of angular frequencies 0.1-100, except at high angular frequencies. This suggests that the elastic response predominates due to the presence of a strong network formed by the cross-linking system. However, at higher frequencies, there is a crossover between G' and G'' values, which indicates the breaking of network structure. In Figure 7 (a), the addition of GO increases both G' and G", but the G' values are strongly modified in the presence of different concentrations of GO due to the strong ionic and hydrogen bonding interaction between GO and the groups present on the CS bathe bone. Our studies demonstrate that we have successfully modified the viscoelastic properties of hydrogels by including GO. Therefore, we can conclude that GO acts as a physical cross-linker due to its strong ionic interaction with the positively charged groups of CS and –COO- groups of GD, as well as its hydrogen bonding interactions, while GD acts as a strong covalent cross-linker.

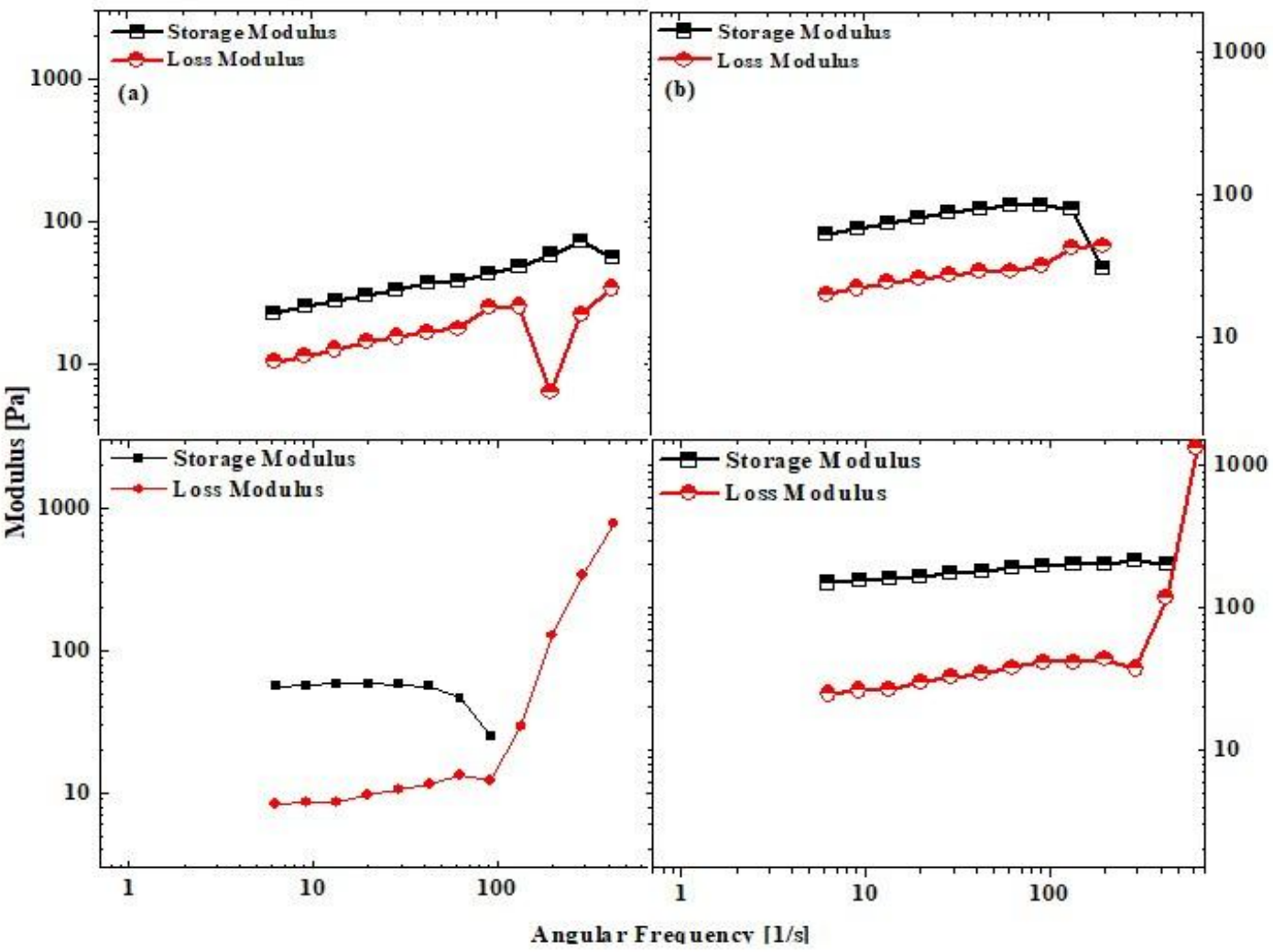

Figure 7:- Frequency sweep plots of CS hydrogels

CONCLUSION

Given the ever-growing and divergent application status of hydrogels, our endeavor and effort in this regard were to carry out the synthesis of Chitosan-based hydrogels. We invested our efforts in the modulation of viscoelastic properties of CS in the presence of dual crosslinker GD and GO. Since Graphene oxide is the best available crosslinker itself we utilized the general properties of GO to form hydrogel with CS. We could formulate two types of hydrogels, one in which we used only GO as a crosslinker, and in a second we used both GD and GO forming a CS-GD+GO hydrogel system. The Hydrogels were formed due to the strong electrostatic interactions between oppositely charged groups between CS and GO sheets and successfully giving a hybrid and dual crosslinked hydrogel involving both covalent crosslinking (GD) and ionic crosslinking (GO). We have explored the rheological properties of hydrogels suggesting

the high property disposition in terms of viscosity and elastic modulus, hence in summary we could manipulate the mechanical behavior of Chitosan-based hydrogels required for a broad spectrum of applications. The SEM analysis shows the presence high porous surface in the presence of GO required for applications like heavy metal sequestration, dye sorption, and sorption of polyaromatic hydrocarbons. What is more, we have also achieved a highly stretchable system due to the reversible nature of interactions. The ionic crosslinking and hydrogen bonding interactions made this hydrogel stretchable with high tensile strength under large deformations which can be ascribed to the hydrogel systems with dual crosslinking.

Funding Not applicable

Declarations Ethics approval and consent to participate are Not applicable

References

1. Enas M. A., Hydrogel: Preparation, characterization, and applications: A review, J. Adv. Res., 6(2), (2015), 105-21.
2. Khan A., Alamry K.A., Recent advances of emerging green chitosan-based biomaterials with potential biomedical applications: A review, Carbohydr. Res. 506, (2021), 108–368.
3. Das N., Tripathi N., Basu S., Bose C., Maitra S., Khurana, S., Progress in the development of gelling agents for improved culturability of microorganisms, Front. Microbiol., 6, (2015).
4. Ullah F., Othman M.B.H., Javed F., Ahmad Z., Akil H.M., Classification, processing and application of hydrogels: A review, Mater. Sci. Eng.: C, 57, (2015), 414-433.
5. Peppas N.A., Hilt J.Z., Khademhosseini A., Langer R., Hydrogels in Biology and Medicine: From Molecular Principles to Bionanotech. 18(11), (2006), 1345–1360.
6. Narayan B., Jonathan G., Miqin Z., Chitosan-based hydrogels for controlled, localized drug delivery. 62(1), (2010), 83–99.
7. Nga H.N D, Quyen T.T., Phung K.L., Anh C.H., Recent developments in chitosan hydrogels carrying natural bioactive compounds, Carbohyd Polym, 294, (2022), 119726
8. Moises B-T., David R-F., Belen A-V., Kenia P., Héctor M., Emilio B., Hydrogels

Classification According to the Physical or Chemical Interactions and as StimuliSensitive Materials . Gels. 7(4), (2021),182;

9. Dominik S., Marta B., Justyna F., Zbigniew D., Antibacterial and Antifungal Properties of Modified Chitosan Nonwovens. Polym. 14(9), (2022),1690.
10. Hamid H., Sara M., Samuel M.H., Alan E.T., Martin W.K., Chitosan based bioadhesives for biomedical applications: A review. Carbohydr. Polym, 15, (2022), 282:119100.
11. Peng F.., Yanbo Z., Dionisio Z-S., Lissette A., Shige W., Chitosan-Based Hemostatic Hydrogels: The Concept, Mechanism, Application, and Prospects. Molecules. 28(3), 2023, 1473.
12. Abd El-Hack M.E., El-Saadony M.T., Shafi M.E., Zabermawi N.M., Arif M., Batiha, Gaber Elsaber; Khafaga, Asmaa F.; Abd El-Hakim, Yasmina M.; Al-Sagheer, Adham A., Antimicrobial and antioxidant properties of chitosan and its derivatives and their applications: A review. Int. J. Biol. Macromol., 164, (2020), 2726–2744.
13. Wang W., Xue C., Mao X., Chitosan: Structural modification, biological activity and application. Int. J. Biol. Macromol., 164(), (2020). 4532–4546.
14. de Sousa Victor R., Marcelo da Cunha Santos A., Viana de Sousa B., de Araajo Neves G., Navarro de Lima Santana L., Rodrigues Menezes R., A Review on Chitosans Uses as Biomaterial: Tissue Engineering, Drug Delivery Systems and Cancer Treatment. Materials, 13(21), (2020), 4995.
15. Hamedi H., Moradi S., Hudson S.M., Tonelli A.E., Chitosan Based Hydrogels and Their Applications for Drug Delivery in Wound Dressings: A Review, Carbohyd. Polym. (2018), S0144861718307690–
16. Ahmadi F., Oveisi Z., Mohammadi S.S., Amoozgar Z., Chitosan based hydrogels: characteristics and pharmaceutical applications, Res Pharm Sci., 10(1), 2015, 1–16.
17. Gheorghita R., Anchidin-Norocel L., Filip R., Dimian M., Covasa M., Applications of biopolymers for drugs and probiotics delivery, Polym. 13, (2021), 2729.
18. Rebitski E.P., Darder M., Chitosan and pectin core–shell beads encapsulating metformin–clay intercalation compounds for controlled delivery, New J. Chem. 44, (2020), 10102–10110.
19. Aranaz I., Alcántara A.R., Concepción Civera M., Arias C., Elorza B., Caballero A.H.,

Acosta N., Chitosan: An Overview of Its Properties and Applications, Polym.13, (2021), 3256.

20. Ardean C., Davidescu C.M., Nemeş N.S., Negrea A., Ciopec M., Duteanu N., Negrea P., Duda-Seiman D., Musta V., Factors Influencing the Antibacterial Activity of Chitosan and Chitosan Modified by Functionalization. Int. J. Mol. Sci. 22, (2021),7449.
21. Rasweefali M.K., Sabu S., Sunooj K.V., Sasidharan A., Xavier K.A.M., Consequences of chemical deacetylation on physicochemical, structural and functional characteristics of chitosan extracted from deep-sea mud shrimp, Carbohydr. Polym. Technol. Appl. 2, (2021), 100032–100043.
22. Amiri H., Aghbashlo M., Sharma M., Gaffery J., Manning L., Basri S.M.M., Kennedy J.F., Gupta V.K., Tabatabaei M., Chitin and Chitosan derived from crustacean waste valorization streams can support food systems and the UN Sustainable Development Goals. Nat. Food, 3, (2022), 822–828.